Journal of Constructional Steel Research 66 (2010) 1467–1482

Contents lists available at ScienceDirect

Journal of Constructional Steel Research

journal homepage: www.elsevier.com/locate/jcsr

Sub-structural pseudo-dynamic performance of two full-scale two-story steel plate shear walls

Chih-Han Lin [b,1], Keh-Chyuan Tsai [a,b,*], Bing Qu [c,2], Michel Bruneau [d,3]

[a] Department of Civil Engineering, National Taiwan University, No. 1, Sec. 4, Roosevelt Road, Taipei, 106, Taiwan
[b] National Center for Research on Earthquake Engineering, No. 200, Sec. 3, Xinhai Road, Taipei, 106, Taiwan
[c] Department of Civil and Environmental Engineering, California Polytechnic State University, San Luis Obispo, CA 93407, United States
[d] Department of Civil, Structural and Environmental engineering, University at Buffalo, Buffalo, NY 14260, United States

ARTICLE INFO

Article history:
Received 22 September 2009
Accepted 24 May 2010

Keywords:
Steel plate shear wall
Tension field
Strip model
Pseudo-dynamic test

ABSTRACT

This paper describes two eight-meter tall and four-meter wide, two-story steel plate shear walls (SPSWs) that were fabricated and tested using sub-structural pseudo-dynamic testing procedures in the National Center for Research on Earthquake Engineering (NCREE). In the Phase I tests, all wall panels were restrained using horizontal tube restrainers on both sides in order to minimize both the out-of-plane displacement and the buckling sound. In the Phase II tests, damaged steel plates were removed and replaced with new plates without restrainers. Both specimens were tested under pseudo-dynamic loads using several scaled ground accelerations. This paper presents primarily the design of the specimen, experimental results, and simplified analytical modeling techniques for Phase I specimen. Results of the Phase I tests show that (1) the SPSW specimen sustained three earthquakes without significant wall fracture or overall strength degradation, (2) the horizontal restrainers were effective in improving the serviceability of the SPSW, (3) the responses of the SPSW can be satisfactorily predicted using the strip model and the tension-only material property implemented in the PISA3D computer program, (4) the energy-dissipating capacity of the SPSW specimen was found to be substantially reduced when it was subjected to the same ground motions again, and (5) if the boundary elements are properly proportioned using the capacity design principle, the equivalent brace model is effective for the response analysis of SPSW buildings subjected to strong ground motions.

1. Introduction

A steel plate shear wall (SPSW) is a lateral force-resisting system that consists of steel panels added as infill to a building's structural frame. A typical SPSW frame structure is shown in Fig. 1. Due to the extreme stiffness and strength of the SPSW frame system when using the thick plates, thin plates are often used in SPSWs. After the infill plate buckles in shear, it is possible to develop diagonal tension field actions, as shown in Fig. 2 [1]. Thus, the SPSW system can dissipate energy through yielding of the infill panels. In recent years, several researchers have confirmed that the SPSW system can be a viable seismic force-resisting system for structures [2–9]. Although the SPSW system can cost-effectively satisfy the lateral stiffness, strength, and ductility requirements for seismic buildings, experimental research on large-scale multi-story SPSW structures is rather limited. Two reduced-scale four-story specimens were tested by Driver et al. [2] and Lubell et al. [4]. Thus, a full-scale two-story SPSW specimen was constructed and tested using pseudo-dynamic procedures at NCREE. This study was a collaborative research project [10] between the National Taiwan University, the NCREE, the University at Buffalo, and the Multidisciplinary Center for Earthquake Engineering Research. The SPSW specimen measured eight meters tall and four meters wide. The thicknesses of the SS400 grade steel plates were 3.0 and 2.0 mm for the first and second stories, respectively. In the Phase I tests, both the top and bottom steel panels (Fig. 3(a)) had horizontal tube restrainers on both sides of the steel plate to minimize out-of-plane displacement and the buckling sound. The specimen was tested under pseudo-dynamic loads using three ground accelerations which were recorded during the 1999 Chi-Chi earthquake and scaled up to represent seismic hazards of 2%, 10%, and 50% probabilities of exceedance, over 50 years. After these tests, there was no

* Corresponding author at: Department of Civil Engineering, National Taiwan University, No. 1, Sec. 4, Roosevelt Road, Taipei, 106, Taiwan. Tel.: +886 2 3366 4318; fax: +886 2 2739 6752.
E-mail addresses: hanklin@ncree.org (C.-H. Lin), kctsai@ncree.org, kctsai@ntu.edu.tw (K.-C. Tsai), bqu@calpoly.edu (B. Qu), bruneau@buffalo.edu (M. Bruneau).
1 Tel.: +886 2 6630 0884; fax: +886 2 6630 0858.
2 Tel.: +1 805 756 5645; fax: +1 805 756 6330.
3 Tel.: +1 716 645 3398; fax: +1 716 645 3733.

0143-974X/$ – see front matter © 2010 Elsevier Ltd. All rights reserved.
doi:10.1016/j.jcsr.2010.05.013

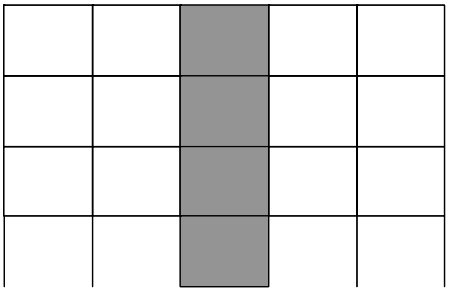

Fig. 1. Typical SPSW frame system.

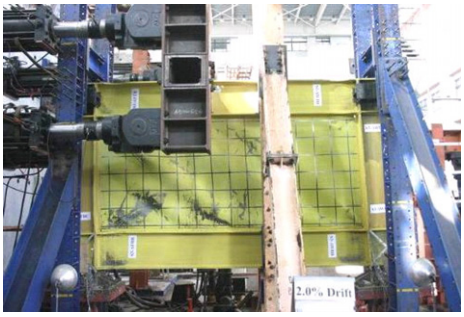

Fig. 2. Tension field actions.

fracture found in the boundary beams and columns. Subsequently, the damaged steel plates were removed and the new plates were installed to the existing moment-resisting frame. However, in the Phase II tests, restrainers were not used (Fig. 3(b)).

The strip model as shown in Fig. 4, consisting of two series of inclined pin-end truss members, has been widely used in the analysis of SPSWs [11,2,5]. In order to simulate the cyclic responses of the thin steel plates after shear buckling, a new material property, named tension-only, is proposed to represent the cyclic responses of the strip. It requires the definition of a significant number of nodes and elements in the analytical model. Therefore, in structural engineering practice, the strip model may not be suitable for the preliminary analysis of a multi-story SPSW. Thus, the simplified equivalent brace (EB) analytical model [11], which uses one single diagonal brace to simulate the monotonic responses of SPSWs, is reviewed. In order to predict the nonlinear cyclic responses of the SPSW using EBs, the method of computing the material properties for the EB is proposed in this paper. The analytical results using a pair of equivalent braces with tension-only material property are also presented in this study. This paper discusses primarily the specimen design, key experimental and analytical results for the Phase I tests. The detailed test and three-dimensional (3D) finite element analytical results associated with the Phase II tests can be found in a separate paper [12].

2. The strip model for the design of SPSWs

The strip model proposed by Thorburn et al. [11] is widely used for the analysis of SPSW frames. In this model, two series of inclined pin-end truss members as shown in Fig. 4 are used to represent the cyclic tension field action in the steel plate. The incline angle α of the strip can be calculated from the following equation [11]:

$$\tan^4\alpha = \frac{1+\frac{Lt}{2A_c}}{1+\frac{h_s t}{A_b}+\frac{h_s^4 t}{360 I_c L}}, \tag{1}$$

where h_s is the story height, L is the bay width, A_b is the beam cross-sectional area, t is the thickness of the plate, and A_c and

Fig. 3. Specimen for (a) Phase I tests and (b) Phase II test.

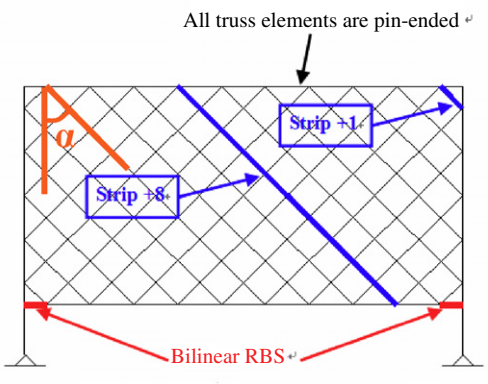

Fig. 4. The strip model.

I_c are the cross-sectional area and moment of inertia of the column, respectively. In a typical interior panel, the upward and the downward components of the tension field will nearly balance one another. Thus, in Eq. (1), the beam flexural strain energy is not included. In past research [2,13], it has been found that the capacity of the SPSWs is not especially sensitive to the angle of inclination. In this study, a more accurate method of computing the incline angle of the strips including the strain energy of all boundary beams has been developed [10], and it is presented in Eq. (2):

$$\tan^4\alpha = \frac{\frac{h}{tL}+\frac{h}{2A_c}+\frac{L^3}{360 I_b}}{\frac{h}{tL}+\frac{h_s^2}{A_b L}+\frac{h_s^5}{360 I_c L^2}}, \tag{2}$$

where I_b is moment of inertia of the boundary beams. It has been found that the incline angle α computed from Eq. (2) is more accurate than Eq. (1) in predicting the tension field direction observed in the tests of large-scale single-story SPSWs [14]. Therefore, Eq. (2) has been used in computing the incline angle of the strips in all the analyses presented in this study. Before the tension field actions develop, the thin steel plate buckles at a very small inter-story drift. Thus, the compressive truss members used in the strip model possesses negligible compressive capacity. For this reason, a tension-only material model was implemented [10] for the PISA3D computer program [15]. The stress versus strain relationships for the material, in tension only, are shown in Fig. 5. This material property represents the response of a typical strip (yielding in tension combined with zero force capacity in compression) developed in a thin steel plate subjected to cyclic strains. Fig. 6 shows the elevation of a single-story SPSW test specimen [14,10] and the analytical model for this specimen is shown in Fig. 4. Fig. 7 compares

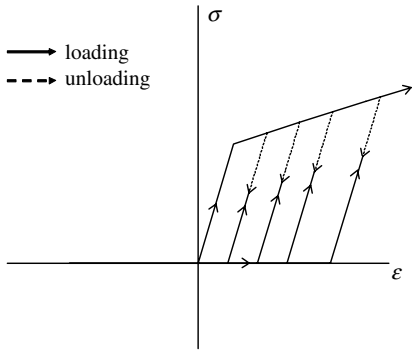

Fig. 5. Stress versus strain relationships of the tension-only material.

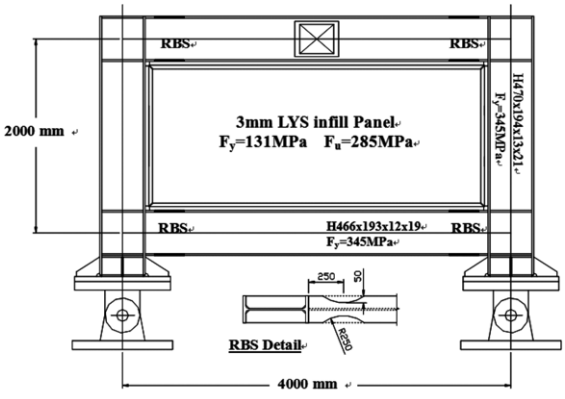

Fig. 6. Single-story SPSW specimen [14].

the test results with the PISA3D simulation results using material that is capable of resisting tensile stresses. The analytical results are consistent with the test results. In addition, the analytical results can be conveniently used to study the deformation demands imposed upon the center and corner of the steel panel. It is evident that the tension field action is substantially more pronounced in the center (e.g. Strip+8 shown in Fig. 6) than in the corner (e.g. Strip+1 in Fig. 6) of the SPSW.

3. Experimental program

Driver et al. [2] cyclically tested a 3.0 m wide and 7.2 m tall, four-story SPSW specimen. In 2000, another reduced-scale four-story specimen was tested using quasi-static procedures [4]. The specimen's width and height were 0.9 and 3.6 m, respectively. Experiments conducted on large-scale multi-story SPSWs have been rather limited. Considering that tests on small-scale specimens may not accurately reflect the seismic performance of a multi-story SPSW frame system, the two-story full-scale SPSW tested in this research is the largest ever tested using pseudo-dynamic procedures and applying realistic earthquake load effects. The specimen design, experimental setup, instrumentation, and pseudo-dynamic test procedures are described in the following sections.

3.1. Design of a two-story prototype building

It is assumed that the lateral force-resisting system of the two-story prototype building includes a steel welded moment frame perimeter with two SPSW frames in the transverse direction. Figs. 8 and 9 describe the floor framing plan, the member sizes of the SWMF, and the 3D perspective of the prototype structure. This two-story prototype building was assumed to be located in the East District in Chiayi City, Taiwan. The design dead load of the floor is 6.87 kN/m^2, and the design live load is 2.45 kN/m^2 for each floor. Based on the latest seismic force requirements for new buildings in Taiwan (ABRI 2002), the design base shear is approximately 22% of the weight of the structure in both directions. Considering the availability of the thin steel plate, SS400 grade steel was chosen for the steel plate shear wall. All the beams and columns in the LFRS are A572 GR 50 steel. The fundamental vibration periods of the building are 0.531 and 0.72 s in the transverse and longitudinal directions, respectively.

Design of the two-story SPSW

It is assumed that the two SPSW frames (steel plate and boundary frame) resist a total of 75% of the lateral design force. In addition, the two boundary columns resist 30% of the lateral force in the SPSW frame. The plate thickness and boundary frame member sizes were chosen based upon recommendations provided by Berman and Bruneau [6]. In order to ensure that the tension field action can be developed, the capacity design method was applied to check the adequacy of the boundary elements. The capacity design of the boundary elements has been proposed by other researchers [1,16]. A simplified but conservative approach has been adopted in this study, as given below.

(1) Assume that all boundary beams and columns are fixed at both ends while they are subjected to the distributed loads from the tension field action as shown in Fig. 10.
(2) The distributed loads acting on the beams and columns are given by the following equations:

$$\text{Top beam: } (W_b)_v = F_y \cdot t_2 \cdot \cos^2 \alpha \tag{3}$$

$$\text{Bottom beam: } (W_b)_v = F_y \cdot t_1 \cdot \cos^2 \alpha \tag{4}$$

$$\text{Middle beam: } (W_b)_v = F_y \cdot (t_1 - t_2) \cdot \cos^2 \alpha \tag{5}$$

$$\text{Column: } (W_c)_h = F_y \cdot t \cdot \sin^2 \alpha, \tag{6}$$

where F_y is the infill plate tension yield stress, t_1 and t_2 are the thicknesses of infill plates in the first and second story, and α is the angle of inclination of the strips.

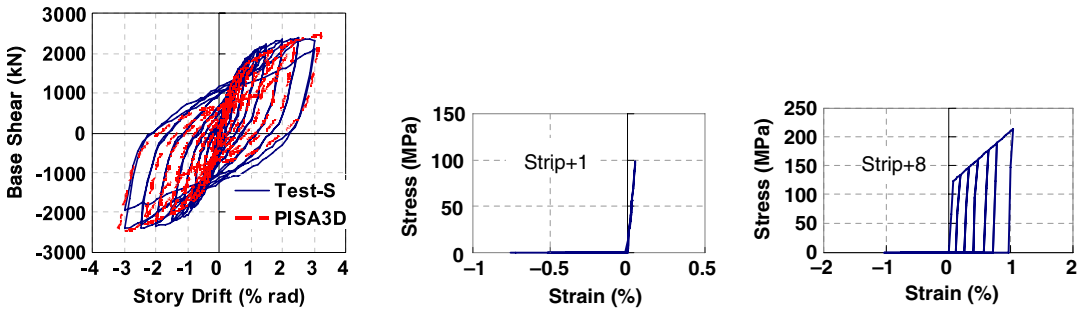

Fig. 7. Single-story SPSW test and analysis results.

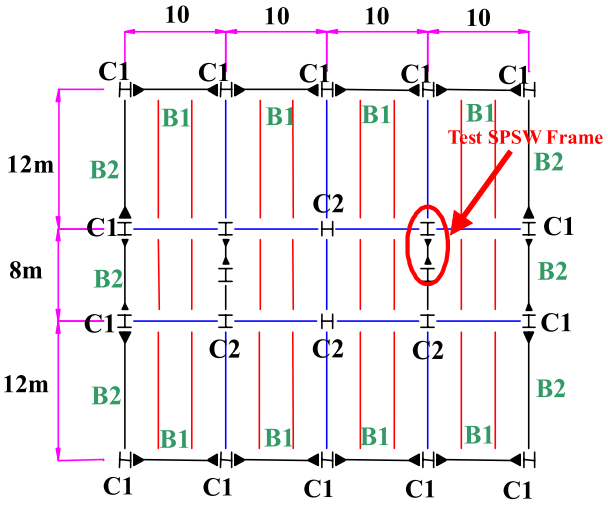

Member	A572 GR50
C1	H400x400x20x35
C2	H 400 x 300 x 18 x 26
B1	H600x200x16x26
B2	H600x200x12x20

Fig. 8. Floor framing plan of the prototype building.

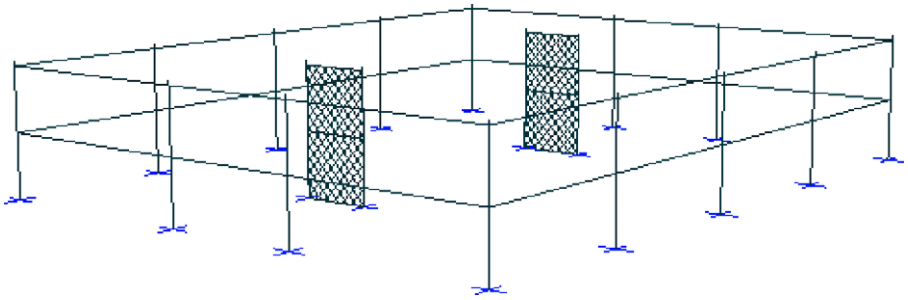

Fig. 9. PISA3D analytical model (strip model).

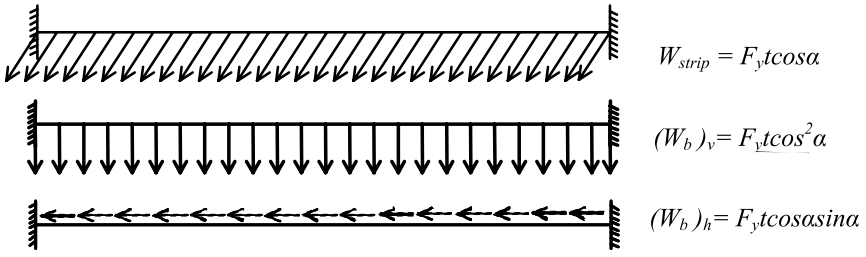

Fig. 10. Beam boundary condition and distributed load.

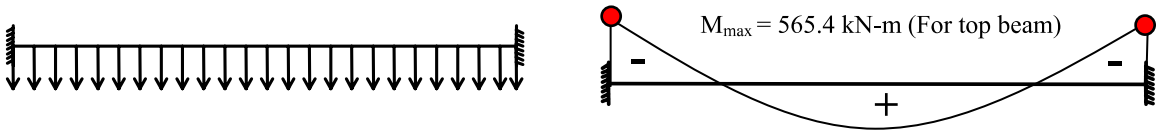

Fig. 11. Moment distribution induced by tension field action.

(3) *Computing the axial and shear force demands in boundary beams*: Considering the effect of material overstrength of the steel plate, the axial and shear force demands on the boundary beams can be calculated from Eqs. (5) and (6):

$$(P_{\max})_{\text{Beam}} = \frac{1}{2}\cdot R_y \cdot W_b \cdot \tan\alpha \cdot L = \frac{1}{2}\cdot R_y \cdot F_y \cdot t \cdot \sin\alpha \cdot \cos\alpha \cdot L \quad (7)$$

$$(V_{\max})_{\text{Beam}} = \frac{1}{2}\cdot R_y \cdot W_b \cdot L = \frac{1}{2}\cdot R_y \cdot F_y \cdot t \cdot \cos^2\alpha \cdot L, \quad (8)$$

where $R_y = 1.5$ is the material overstrength factor of the steel plate.

(4) *Computing the flexure demands in boundary beams*: It is assumed that the flexural demand on the boundary beams and columns can be evaluated from two components ($M_{\text{FrameAction}}$ and $M_{\text{TensionField}}$). $M_{\text{TensionField}}$ is the maximum moment induced by the distributed loads on the boundary beams (Fig. 11). Thus, the maximum moment applied to the beam ends due to the tension field action can be evaluated as

$$M_{\text{TensionField}} = \frac{1}{12}\cdot R_y \cdot W_b \cdot L^2 = \frac{1}{12}\cdot R_y \cdot F_y \cdot t \cdot \cos^2\alpha \cdot L^2. \quad (9)$$

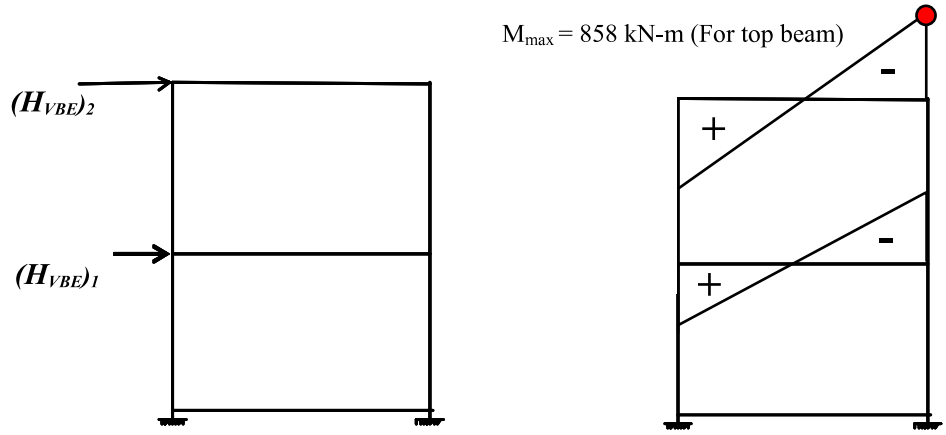

Fig. 12. Moment distribution due to H_{VBE}.

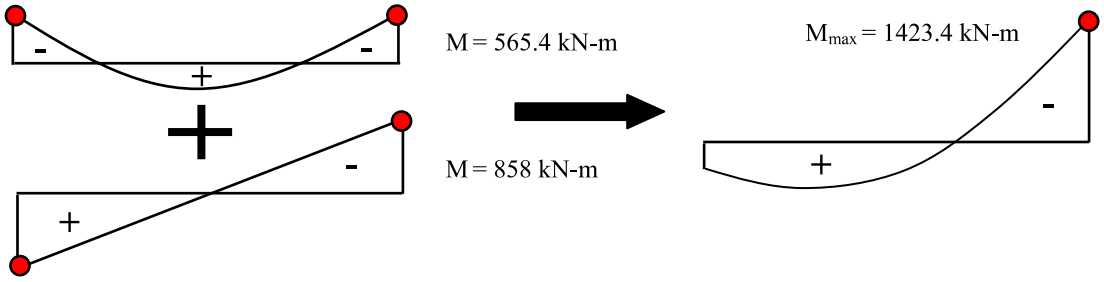

Fig. 13. Moment distribution due to the tension field and frame action.

The maximum shear force in the steel panel can be computed from the following equation:

$$H_{\text{strip}} = \frac{1}{2} \cdot R_y \cdot F_y \cdot t \cdot L \cdot \sin 2\alpha. \tag{10}$$

As assumed previously, the two boundary columns resist 30% of the total SPSW frame lateral force. Thus, in this study, the maximum shear force carried by two vertical boundary columns in each story $(H_{\text{VBE}})_i$ can be estimated from the maximum lateral force $(H_{\text{strip}})_i$ resisted by the steel panel in each story, as shown below:

$$(H_{\text{VBE}})_2 = \frac{3}{7}(H_{\text{strip}})_2 = \frac{3}{14}\Omega_s \cdot F_y \cdot t_2 \cdot L \cdot \sin 2\alpha \tag{11}$$

$$\begin{aligned}(H_{\text{VBE}})_1 &= \frac{3}{7}(H_{\text{strip}})_1 - (H_{\text{VBE}})_2 \\ &= \frac{3}{14}\Omega_s \cdot F_y \cdot (t_1 - t_2) \cdot L \cdot \sin 2\alpha.\end{aligned} \tag{12}$$

It is assumed for simplicity that the boundary frame remains elastic even during severe earthquakes. Thus, the peak bending moments in the boundary elements due to the frame action ($M_{\text{FrameAction}}$) can be obtained from an elastic frame analysis by applying the lateral force H_{VBE}, as shown in Fig. 12. The total flexural demand on the boundary beams can be computed from the superposition of $M_{\text{FrameAction}}$ and $M_{\text{TensionField}}$ (Fig. 13).

(5) *Computing the force demands in boundary columns*: The column shear and flexure demands can be determined using the same procedure similar to those stated in Steps 3 and 4. However, the axial force demands in the column caused by the overturning of the frame action must be added to those induced by the steel panel.

After completing the capacity design, a 3D analytical model was constructed. The elastic analysis was used to check the ratio of the two boundary column shear and the total story shear against the initial assumption. Iterations of these procedures were required until convergence. In the specimens, the aforementioned force demand to capacity ratios (DCRs) of all the boundary elements was kept under 0.9. The thicknesses of the SS400 grade steel plates were 3.0 and 2.0 mm for the first and second stories, respectively. The material property of the SS400 grade steel is similar to that of A36. The nominal yield strength is 245 MPa. The actual yield strengths for the steel plates were 335 MPa (3.0 mm) and 338 MPa (2.0 mm). The 2.24 m wide, 75 mm thick concrete, over the 75 mm deep metal deck concrete slab, was constructed in both floors. Detailed member sizes are shown in Fig. 14. In order to reduce the buckling sounds and minimize the out-of-plane buckling of the steel panels, these panels were restrained by three horizontal restrainers on both sides of the infill plate in each story. The restrainer has been designed by considering a uniformly distributed out-of-plane tributary load equivalent to 3% of the SPSW maximum shear [14]. The sizes of the tube restrainers were HSS125 × 75 × 4 mm and HSS125 × 75 × 2.3 mm for the first and second stories, respectively. Both ends of each restrainer were connected to the column flange using a slotted joint. After the Phase I tests, the damaged infill plate was replaced by new steel panels of the same grade and thickness. In order to study the seismic performance of the unrestrained SPSW, no restrainer was installed in the Phase II tests.

3.2. Experimental setup

The SPSW column base was bolted to a 100 mm thick steel plate anchored to the floor using 69 mm diameter high-strength steel rods. The arrangement of the actuators in each floor is shown in Fig. 15. Three 980 kN actuators for each floor were used in the plane direction of the SPSW. In order to prevent out-of-plane displacement, two servo-controlled actuators for each floor were used as lateral supports. Three SPSW in-plane actuators in each floor were attached to a transfer beam. Each transfer beam was connected to two edge beams (H150 × 150 × 7 × 10 mm) at the two edges of the concrete slab (Fig. 15). For simulation of the gravity

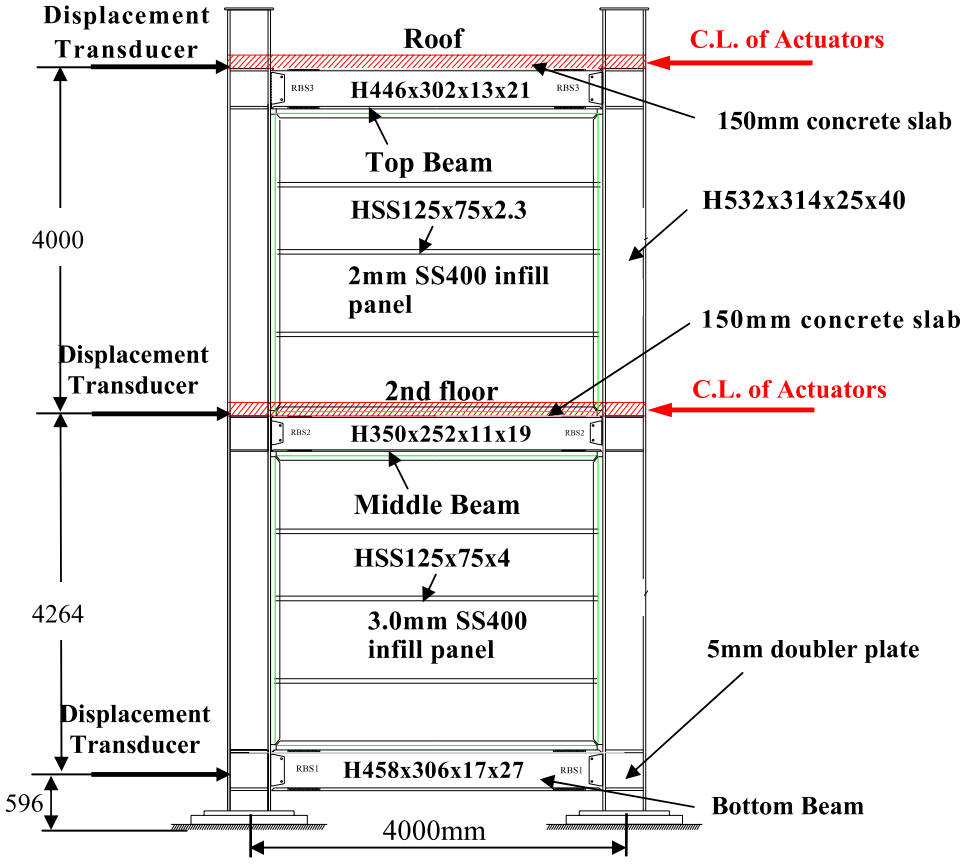

Fig. 14. Elevation of the two-story SPSW specimen.

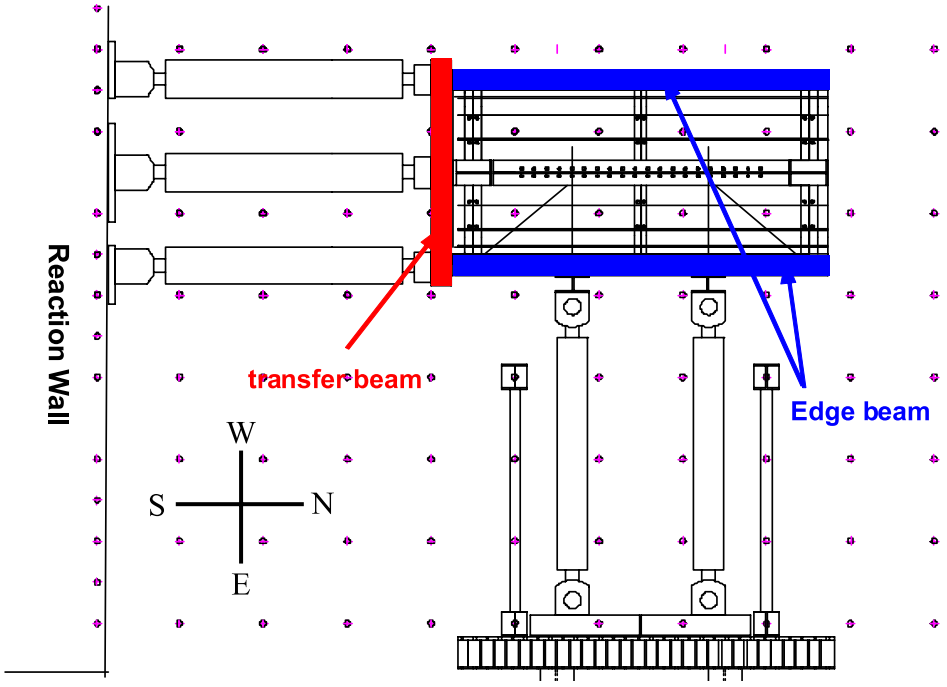

Fig. 15. Plane view of the experimental setup.

load effects, a total of 1400 kN gravity load was applied using two post-tension rods attached to a cap beam over the column top (Fig. 3(a)). The post-tension rods were anchored to the strong floor using hinge supports. Thus, the device of gravity applying can permit the specimen to sway freely.

3.3. Instrumentation

In order to record the response of the specimen during the tests, several types of displacement transducer were installed. These include the following.

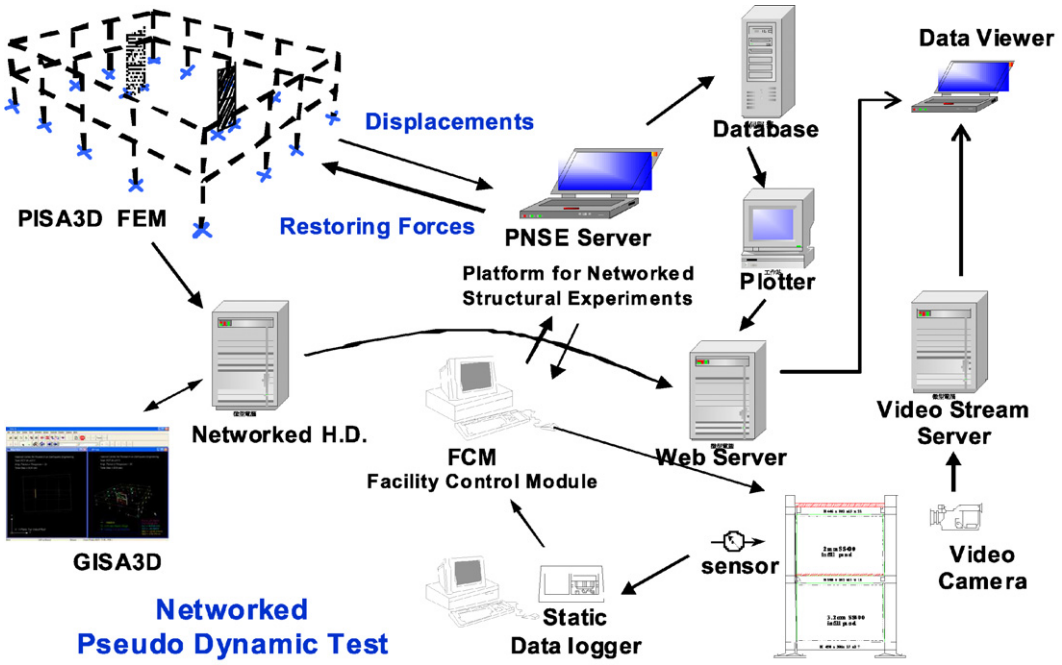

Fig. 16. Networked pseudo-dynamic process.

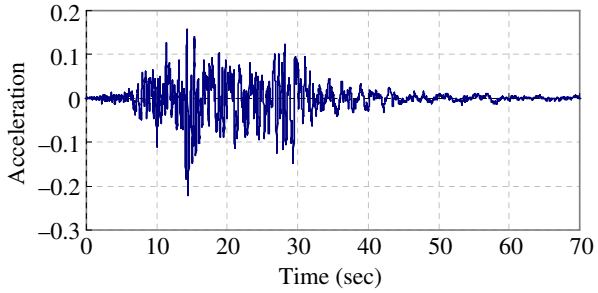

Fig. 17. Original ground acceleration time history.

(1) Strain gauges. Strain gauges were attached to the flanges and webs of the boundary beams and columns. Strain gauges were not placed on the steel panel.
(2) Displacement transducers (LVDTs, dial gauges, PI displacement transducers and Tempsonics). A total of 56 displacement measuring devices were utilized in the tests. The LVDTs were oriented on both sides of the specimen at the same angle as the tension strips in the analytical model. In each story, 12 LVDTs were installed, six in the tension direction and six in the compression direction. Additional LVDTs were placed horizontally along the height of the column. The dial gauges were placed vertically along the beam span. In each beam-to-column joint, the PI displacement transducers were placed diagonally in the panel zone. Temposonics were used to measure the in-plane displacements of both floors.
(3) Rotation transducers (tiltmeters). All tiltmeters were located near the beam-to-column joints to measure the rotation of the boundary beams and columns. During the tests, the static acquisition system was used for data collection. The total number of experimental data channels was 203.

3.4. Networked pseudo-dynamic testing techniques

During the Phase I tests, several computers were networked to conduct the hybrid tests. The various tasks included computing the target displacements (analysis engine), driving the servo-controller (facility control module), performing data acquisition, and distributing experimental and video data to Internet viewers. A schematic of the pseudo-dynamic test is shown in Fig. 16. In this study, the PISA3D computer program was used as the analysis engine. In the PISA3D model, the SPSW frame is considered as a two degree-of-freedom (DOF) stick model which represents the two-story specimen. The initial stiffness of the specimen was measured and entered into the analysis engine to compute the two target displacements. Detailed architecture of the networked hybrid experiments developed at the NCREE has been previously documented [17].

4. Phase I tests

In the Phase I tests, the specimen was examined using pseudo-dynamic test procedures and a Chi-Chi earthquake ground motion record scaled up to represent seismic hazards of 2%, 10%, and 50% probability of exceedance over a 50-year period. For the purpose of discussion, these hazards are denoted as 2/50, 10/50 and 50/50 earthquake events. The original ground acceleration record is TCU082EW, as shown in Fig. 17. The test sequence and ground motion characteristics are shown in Table 1. Before Test 1, severe cracking of the west-side concrete slab occurred in the second floor at the time step of 24.47 s. At that moment, significant buckling was observed in the steel plate shear walls in both stories. However, the test had to be suspended so that the concrete slab could be repaired. In order to observe the seismic performance of the SPSW system with severely buckled steel plates, the same ground motion was adopted in the subsequent test (named Test 1) after repairing the west-side concrete slab in the second floor. The above interrupted test was named the suspend test (ST). The subsequent three hybrid tests were completed without interruption.

After the successful completion of Test 1, it was found that significant buckling (Fig. 18) and a number of small cracks (Fig. 19) had occurred in the steel plate in both stories. Significant yielding of the boundary members was observed during the test. It is described as follows. At time step 6.68 s, slight yielding was found in the bottom beam web (Fig. 20(a)). At time step 9.97 s, significant

Table 1
Test schedule.

Phase I test: restrained steel plate shear wall		
	Excitation	Hazard level
Test 1	Chi-Chi (TCU082EW)	2% in 50 years (PGA = 0.67g)
Test 2	Chi-Chi (TCU082EW)	10% in 50 years (PGA = 0.53g)
Test 3	Chi-Chi (TCU082EW)	50% in 50 years (PGA = 0.22g)

Fig. 18. First-story steel plate buckling.

Fig. 19. Cracks in the steel plate.

yielding was found at both ends of the middle beam, as shown in Fig. 20(b). At time step 17.15 s, yielding was evident on the top beam web at the middle span and both ends, as shown in Fig. 20(c)–(d). In addition, significant yielding was observed on the east column web (Fig. 20(e)) and flange (Fig. 20(f)) above the bottom beam elevation at time step 24.67 s. After Test 1, Tests 2 and 3 imposed the 10/50 and 50/50 hazard level earthquake loads, and were conducted without interruption. After the three Phase I tests, it was found that the SPSW had severely buckled and significantly cracked. However, no fracture was evident in the boundary beams and columns. In addition, there was no yielding or fracture observed on the steel tube restrainers. Thus, after the Phase I tests, it was decided that the damaged steel panels would be replaced with new ones. There were larger out-of-plane displacements in the SPSW in the Phase II tests than those in Phase I. In the Phase II tests, no restrainer was used, and the overall lateral response of specimen was similar to the response during Phase I. The maximum out-of-plane deformation of the steel infill was 50 and 250 mm for the Phase I and Phase II tests, respectively. Additionally, the sound due to steel panel buckling during the Phase II tests was also louder than during the Phase I tests. It is evident that the use of restrainers in the SPSW can effectively reduce the magnitude of the buckling sound and the out-of-plane displacement of the steel panel. Additionally, if the detail of the restrainers processed the proper design, the restrainers can effectively reduce the force demands in beams and columns. The smaller member size can be chosen as boundary elements [16]. During the two phases of testing, all the key analytical predictions and experimental responses were broadcasted from a website (http://exp.ncree.org/spsw).

5. Phase I experimental and analytical results

5.1. PISA3D analytical model for the two-story SPSW specimen

In this study, the PISA3D response history analyses were performed on the complete two-story prototype structure model including the perimeter MRF and the two SPSWs. For each SPSW frame, a total of 48 strips (12 strips for each story in each direction) with inclined angles of $\pm 41^\circ$ were constructed. The complete 3D analytical model of this two-story building is shown in Fig. 9. Because the steel panels in the SPSWs were represented using two series of strips in each direction, the initial stiffness of SPSWs could be overestimated. Therefore, the Young's modulus of the strip material should be reduced to one half for evaluating the fundamental periods of the SPSWs. The aforementioned material (assuming tensile stresses only) was adopted for all strips in order to represent the entire infill panel. All beam and column members in the MRF and boundary frame of the SPSW adopted the bilinear material model for the beam–column element. The tensile coupon strengths (Table 2) of the steel plates and the boundary beams and columns were incorporated into the analytical model. These coupon strengths were obtained through static pulling tests. The two-story SPSW specimen was tested using pseudo-dynamic loads with a speed about 100 times slow of the real time. Therefore,

Table 2
Material coupon test results.

		Positions of sampling	Thickness (mm)	f_y (MPa)	f_u (MPa)
Steel	Panel (SS400)	1F steel infill	3	338	482
		2F steel infill	2	335	412
	Beam (A572)	Base beam web	19	285	480
		Base beam flange	28	355	487
		Middle beam web	12	505	626
		Middle beam flange	19	476	581
		Top beam web	13	305	460
		Top beam flange	22	354	517
	Column (A572)	Column web	25	377	505
		Column flange	40	363	544
Concrete		$f'_c = 27.5$ MPa			

(a) Bottom beam web yielding.

(b) Middle beam web yielding.

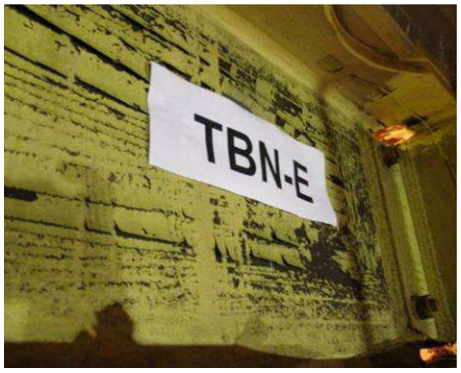

(c) Top beam web yielding.

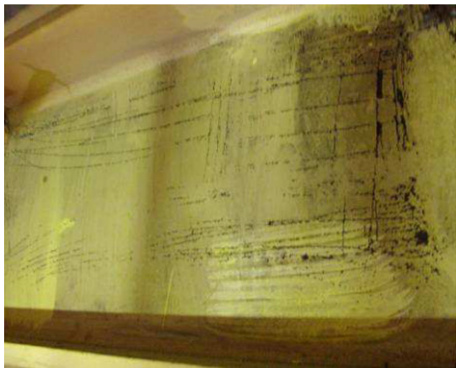

(d) Top beam web yield (middle span).

(e) Column web yielding.

(f) Column flange yielding.

Fig. 20. Yielding of boundary frame during Phase I tests.

strain rate effects were not considered in the analytical model. If real-time hybrid tests could be performed, it would be necessary to investigate the strain rate effects in the following. Assuming a sinusoidal vibration and the maximum inter-story drift to be 0.025 rad for the prototype building with a dominant period of 0.531 s, the maximum strain rate of the strips would be about 0.097 s^{-1}. However, in past research [18], it was found that the yield stress would be influenced by the increase of the strain rate, especially when the strain rate was greater than 0.1 s^{-1}. Thus, it appears that if real-time hybrid tests had been conducted, the strain rate effects could be neglected in the analytical simulation. In this 3D analytical model, the yield strength of the tension-only material used for the steel panels was 370 MPa and 335 MPa in the first and second stories, respectively. Additionally, the post-yield modulus of the tension-only material was specified as 1% and 0.8% of the Young's Modulus for the steel panel in the first and second stories, respectively. Considering the depth of the SPSW boundary members, three rigid ends were specified as the member ends in the analytical model, as shown in Fig. 21(a). A similar approach was adopted when modeling the beams and columns in the perimeter MRF. In the SPSW specimen, the bottom ends of the column were stiffened and anchored on 100 mm thick anchor plates. Thus, the rigid member end offsets were also considered, as shown in Fig. 21(b).

5.2. Discussion of the test and analytical results

Experimental energy dissipation responses

Fig. 22 shows the relationship between the experimental inter-story drift and the story shear of the SPSW for the three consecutive earthquake events (2/50, 10/50 and 50/50). The test results (Fig. 22(a)) confirm that the significant nonlinear energy dissipation responses of the SPSW under the completed 2/50 event were evident. Figs. 23–24 show the story shear versus inter-story

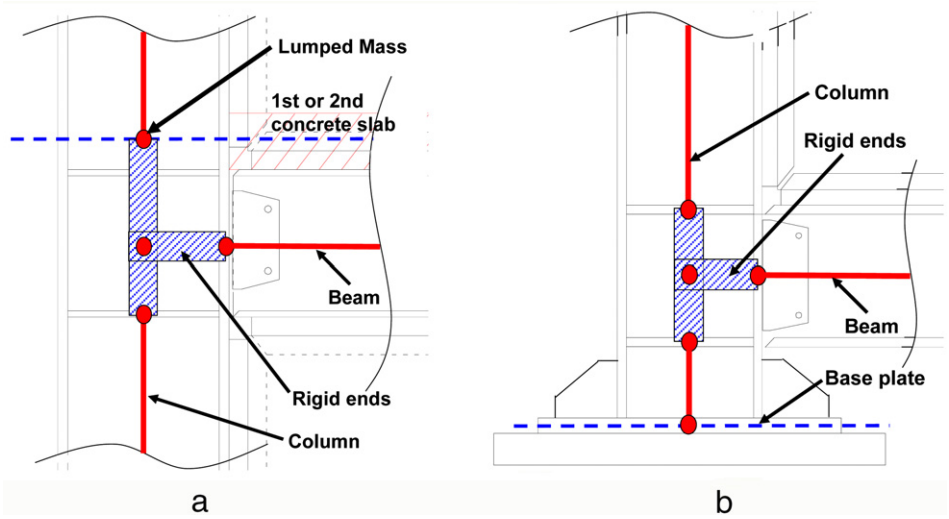

Fig. 21. Modeling methods for (a) beam-to-column connection, (b) column base.

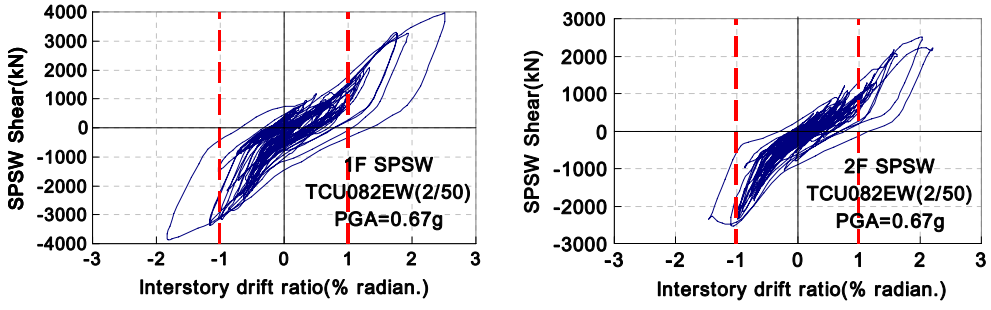

(a) 2/50 event.

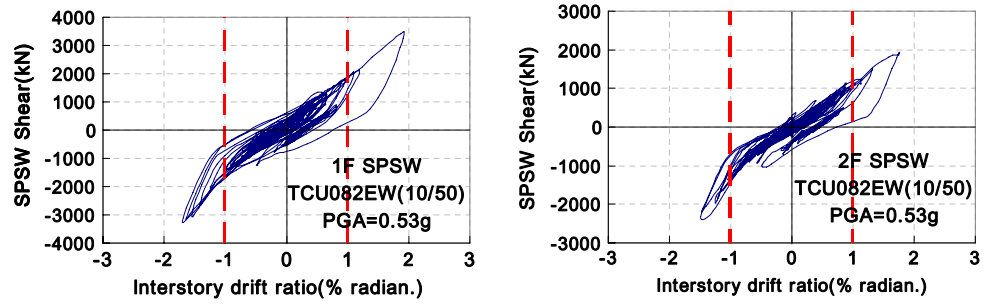

(b) 10/50 event.

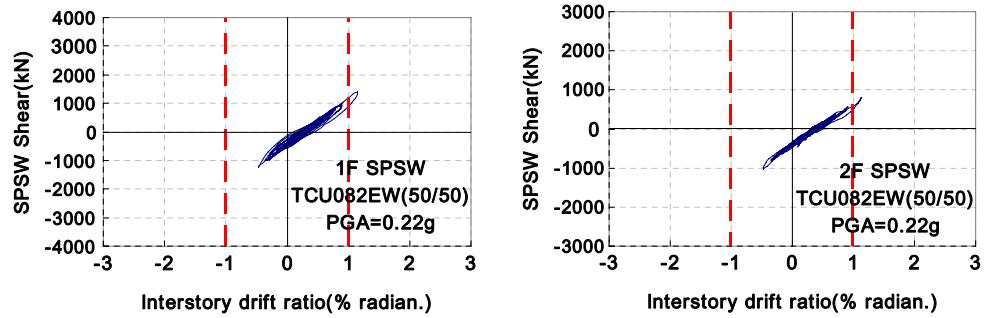

(c) 50/50 event.

Fig. 22. Inter-story drift ratio versus story shear relationships of Phase I tests.

drift relationships and the total accumulated energy dissipation time history for both the suspended test (ST) and Test 1. From Fig. 23, it was determined that the response difference of the two tests is substantially more pronounced when the inter-story drift values are small (between +0.01 to −0.01 rad). From Fig. 23, it is evident that the peak inter-story drift in Test 1 was substantially

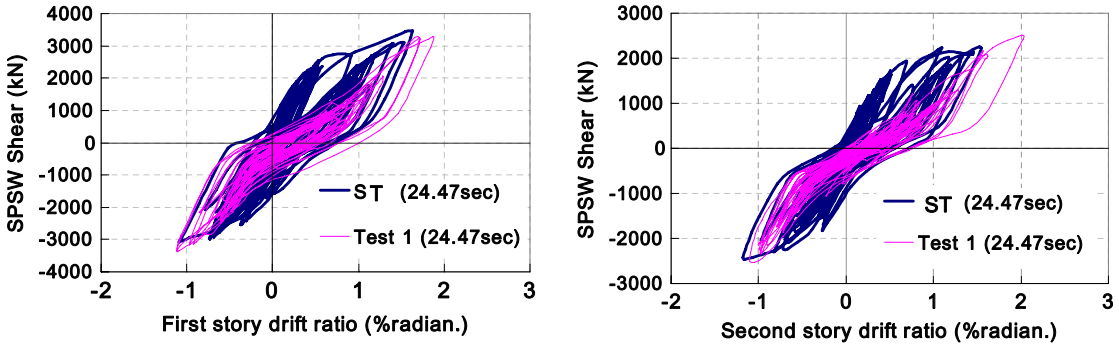

Fig. 23. Story drift versus story shear relationships for the suspended test and Test 1.

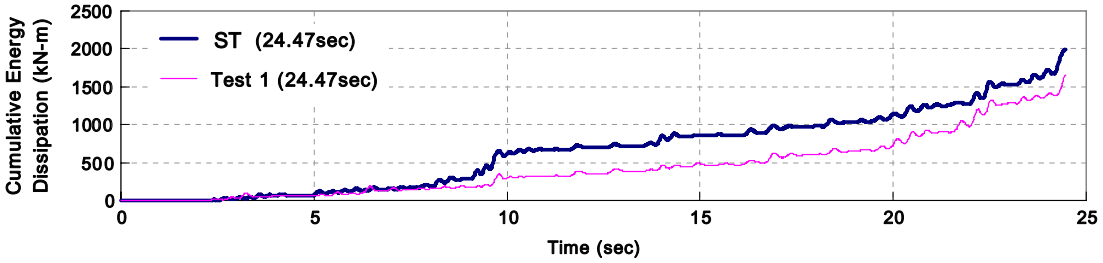

Fig. 24. Total accumulated energy dissipation for the suspended test and Test 1.

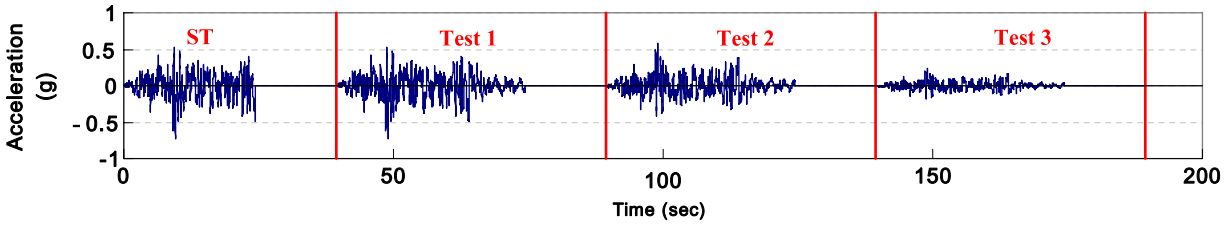

Fig. 25. Continued earthquake ground accelerations used in the analysis.

greater than in the suspended test. However, it can be found in Fig. 24 that the energy dissipated in the SPSW in the first 24.47 s of the 2/50 ground motions is substantially smaller in Test 1 than in the suspended test. This suggests that the SPSW may need to undergo larger drifts to effectively resist a strong aftershock after a strong earthquake. This phenomenon occurs due to the fact that the inelastic tension field action had developed in the ST after the steel panel buckled. Therefore, it required the SPSW to displace further to stretch the buckled steel panel before the tension field action could be regained. A similar trend of SPSW responses was found in Tests 2 and 3 (Fig. 22(b) and (c)). Within the same inter-story drift interval (between −0.01 and +0.01 rad), it was found that the energy dissipation response of the SPSW during the 10/50 and 50/50 events was less pronounced than that found in Test 1 and the ST.

Analytical predictions of floor displacements and story shears

Based on the above discussion of energy dissipation performance of the SPSW during each test, it is evident that the nonlinear response of the SPSW was strongly affected by the existing strain history of the steel infill. Thus, in order to effectively compute the seismic response of the SPSW, four ground accelerations applied in the ST and Tests 1 to 3 were linked together. However, between each ground motion record, 15 s of zero value acceleration was inserted into the time history analysis, as shown in Fig. 25. Fig. 26(a) and (b) present the experimental and analytical floor displacement time history response for the ST and Test 1, respectively. It was found that the displacement response can be predicted reasonably accurately by using the two-way strip model and the tension-only material implemented for the PISA3D program. It is shown in Fig. 22(a) and (b) that the experimental peak story drifts in Tests 1 and 2 are 0.025 and 0.02 rad, respectively. Fig. 27(a) and (b) show the story shear responses of the SPSW during the ST and Test 1, respectively. It was found that the trend of the base shear time histories can be simulated reasonably accurately. Fig. 28 presents the analytical ratio between the shear force carried by all strips and the base shear of the entire SPSW. From Fig. 28, it can be found that maximum ratio is 0.67 when the first story drift reaches 0.003 rad. This shear force ratio agrees rather well with the assumption made in the preliminary design of the SPSW specimen. It can be found in Fig. 28 that the lateral force carried by the steel infill reduces as the story drift increases.

Responses of tension strips

In order to gain insight into the response of the infill steel at various locations, several displacement transducers (LVDTs) were installed in opposite directions on both sides of the steel infill, as illustrated in Fig. 29. Fig. 30 shows the inclined strain versus story shear relationships for the ST and Tests 1 to 3. The inclined strains were computed by dividing the LVDT responses of LVDT-6U and LVDT-6L (Fig. 29) by the gauge distance. It is shown in Fig. 30 that when the inclined strain reaches 0.006 in subsequent earthquake excitations, the story shear resistance was significantly degraded from the first test (ST) to the last test (Test 3). As demonstrated in the 0.006 LVDT-6U strain, the shear resistance was reduced from 2131, to 1440, then to 1267 and 757 kN. In order to evaluate the steel infill strains computed from the analytical model, the responses of Strip-2L and Strip-6L (Fig. 29) were investigated. Fig. 31 compares the experimental inclined strain computed from

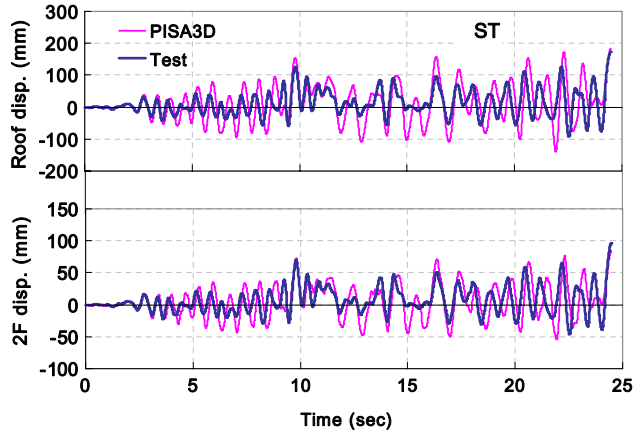

(a) ST.

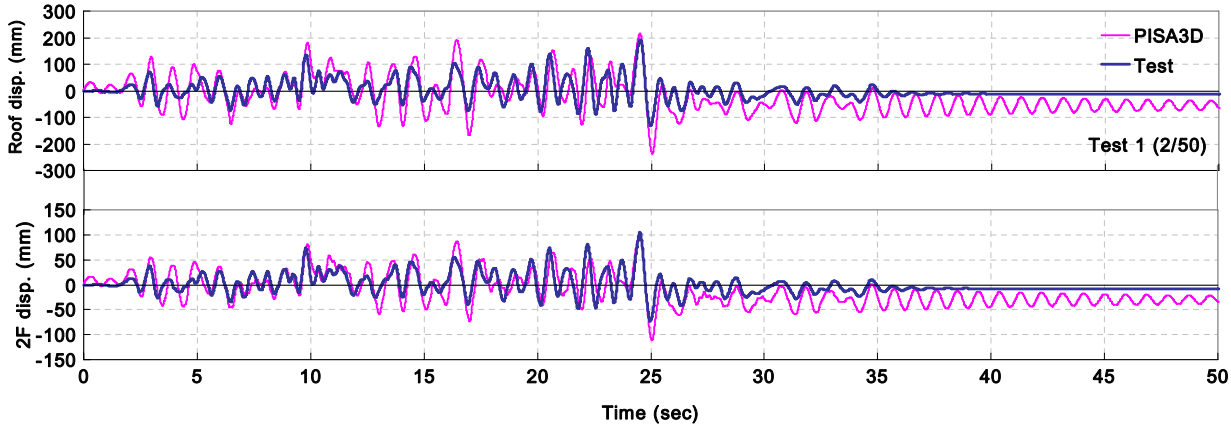

(b) Test 1.

Fig. 26. Story displacement time history responses of ST and Test 1.

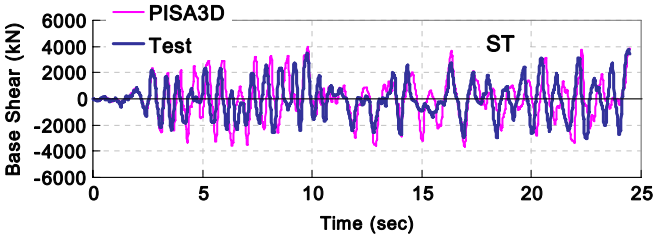

(a) Suspended test.

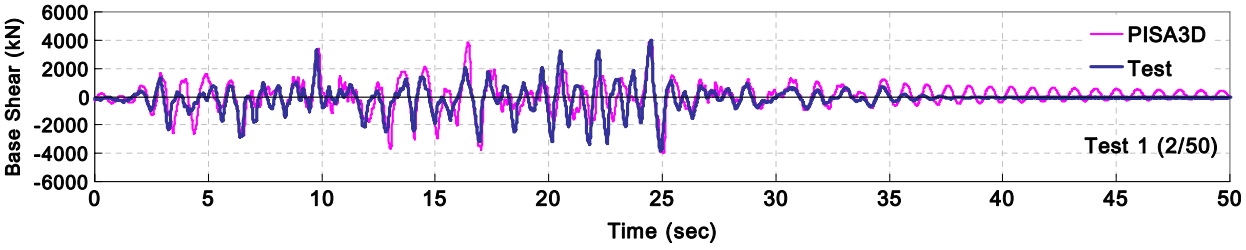

(b) 2/50 events.

Fig. 27. Story shear time history responses of the suspended test and Test 1.

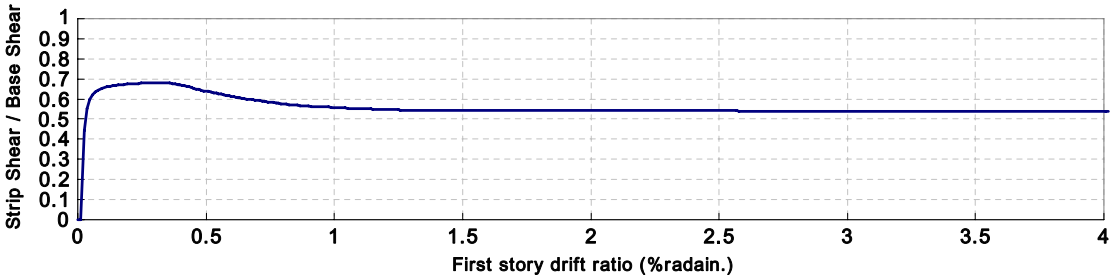

Fig. 28. Ratio of shear forces carried by the steel infill and the total SPSW shear.

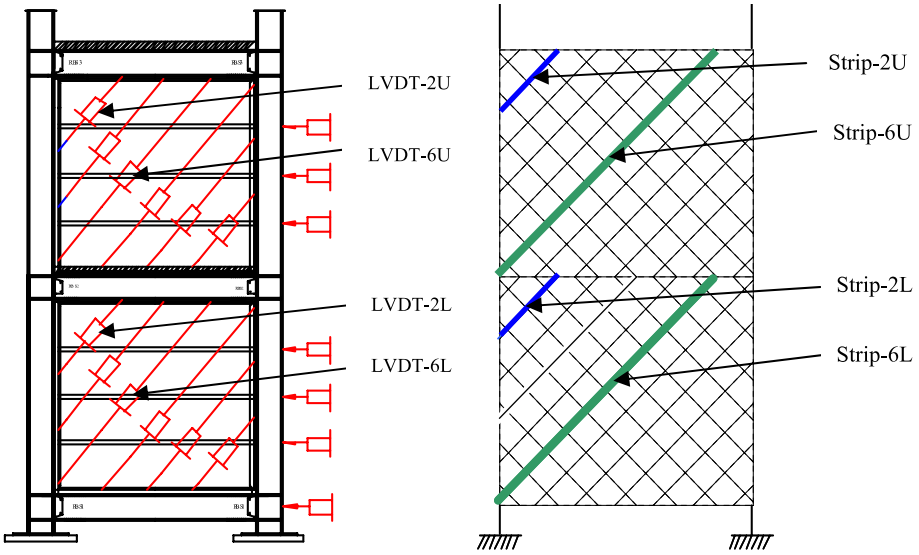

Fig. 29. Identifications of LVDTs and analytical strips.

LDVT-6L and analytical Strip-6L. It confirmed that the strip model satisfactorily predicts the inclined strain history near LVDT-6L. Fig. 32 compares the experimental inclined strains computed from LDVT-6L and LVDT-2L. It is found that the tension field strains in the center of the steel infill were greater than those in the corner. This phenomenon was also observed by other researchers which worked on the seismic behavior of various aspects of SPSWs [2–5,7,8,16].

Equivalent brace model for the two-story SPSW specimen

As noted previously, the floor displacement and story shear responses of the SPSW can be satisfactorily predicted using the strip model and tension-only material. However, the strip model may not be suitable for the preliminary analysis of a multi-story SPSW as it requires the definition of a significant number of nodes and elements. Thus, a simplified model using the equivalent brace (EB) was investigated in this study. The EB model was first proposed by Thorburn et al. [11]. In their EB model, a single diagonal brace is used to represent the steel infill and simulate the cyclic responses of the SPSW. Assuming that the EB and strips have the same overall lateral stiffness, the cross-sectional area of the equivalent brace must be [11]

$$A_{\mathrm{EB}} = \frac{tL\sin^2 2\alpha}{2\sin\theta\sin 2\theta}, \tag{13}$$

where t is the thickness of the infill plates, α is the angle of inclination of the strips, and θ is the angle of inclination of the EB. In order to analyze the nonlinear response of the SPSW using the EB model, this paper further derives the material yield strength for the EB from the assumption that the horizontal yielding force of the EB is the same as the horizontal yield strength of all strips. Assuming that all strips fully yield in tension and that the boundary frame remains elastic, the yield shear force H_{strip} can be obtained from Eq. (8). If the EB yields, the horizontal force component of the EB must be $P_{\mathrm{EB}}\sin\theta = (F_y)_{\mathrm{EB}}A_{\mathrm{EB}}\sin\theta$. Thus, the yield stress of the EB material can be computed from $P_{\mathrm{EB}}\sin\theta = H_{\mathrm{strip}}$:

$$(F_y)_{\mathrm{EB}} = F_y\frac{\sin 2\theta}{\sin 2\alpha}, \tag{14}$$

where F_y is the infill plate tension yield stress. Fig. 33 shows a 3D view of the analytical model using four EBs for each SPSW in the two-story prototype building. In this model, the brace areas are 8890 and 6340 mm^2 for the first and second stories, respectively. The tension-only material was used in each EB. The yielding strengths were 374 and 338 MPa for the EBs in the first and second stories, respectively. The corresponding fundamental periods are respectively 0.538 and 0.531 s when using the EB model and the strip model. Fig. 34 presents the analytical roof displacement and base shear time history responses (for Test 1) using both the strip and the EB models. Fig. 34 shows that the analytical response computed using the strip model and the EB model are almost equivalent. Similar analytical results were also presented in other research [16]. This strongly suggests that the EB model can be effectively used for the preliminary design and global seismic response analysis of properly proportioned SPSW buildings. However, it must be recognized that this model cannot be used to design a frame's beams and columns as it fails to capture the correct moment diagrams on these members (i.e. missing the essential pulling effect of the yielding strips). The boundary elements should be chosen according to the capacity design methods.

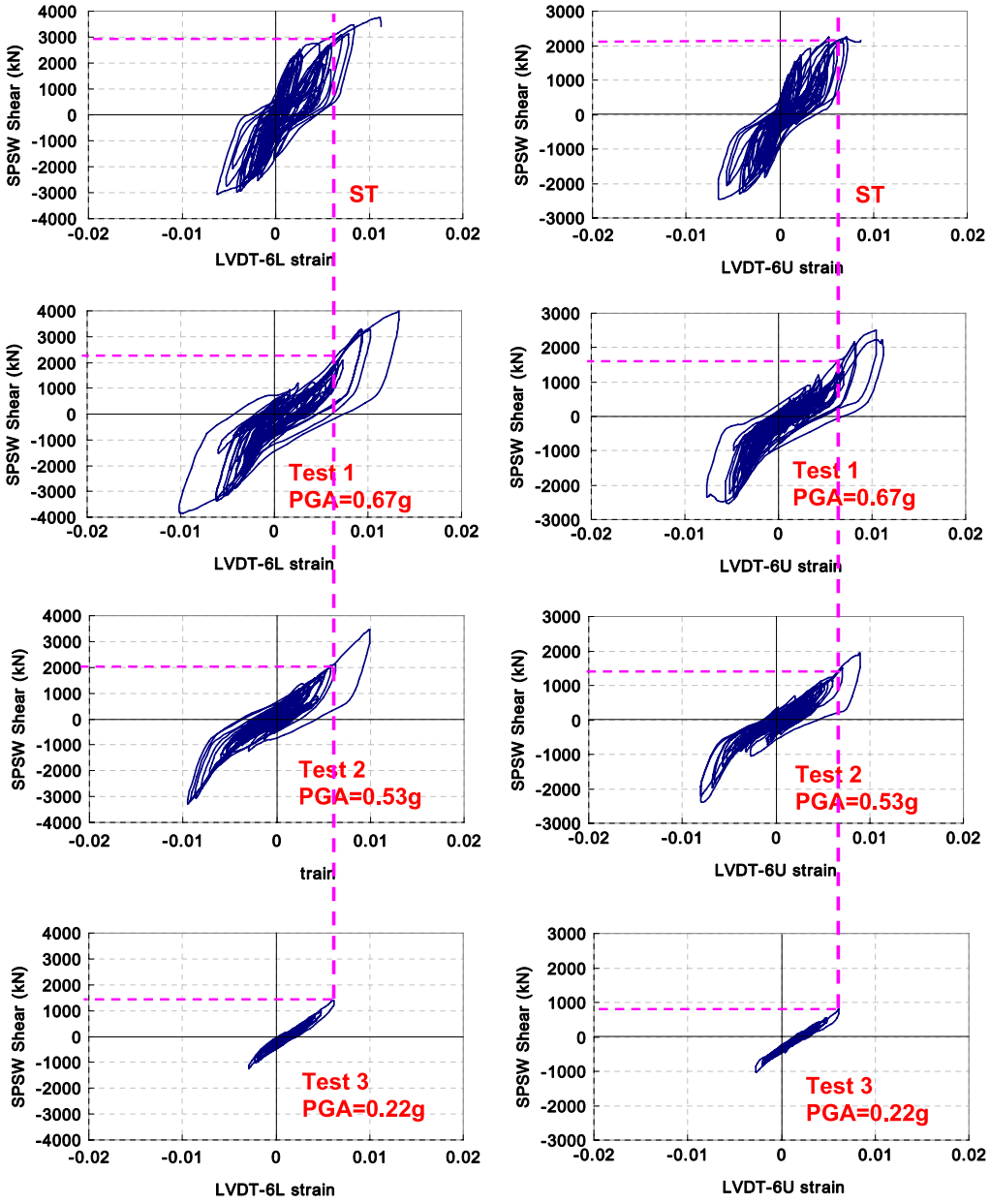

Fig. 30. The strain in the longest tension strip (LVDT-6) versus the SPSW shear relationships for the Phase I tests.

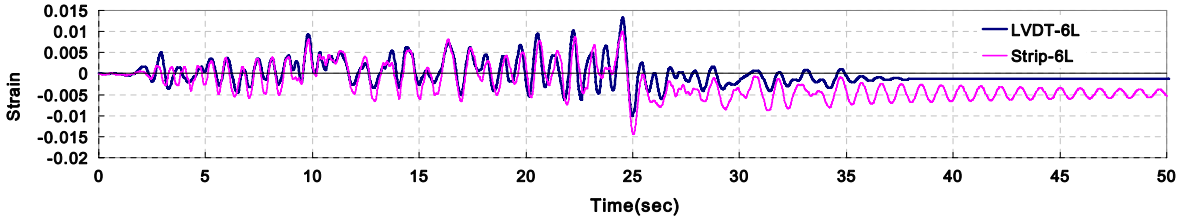

Fig. 31. Responses of LVDT-6L and Strip-6L under the 2/50 event.

6. Conclusions

Based on the experimental and analytical results, the following conclusions and recommendations are made.

- The cyclic response of a single-story SPSW can be satisfactorily simulated using the dual-strip model and tension-only material implemented in the PISA3D computer program.
- During the Phase I tests (with restrainers), the maximum out-of-plane displacement of the steel infill was only about 50 mm, while the out-of-plane displacement in Phase II tests (without restrainers) was 250 mm. In addition, the buckling sounds in the Phase II tests were significantly louder than in Phase I. This suggests that the restrainers can effectively reduce out-of-plane displacements and improve the serviceability of SPSW.

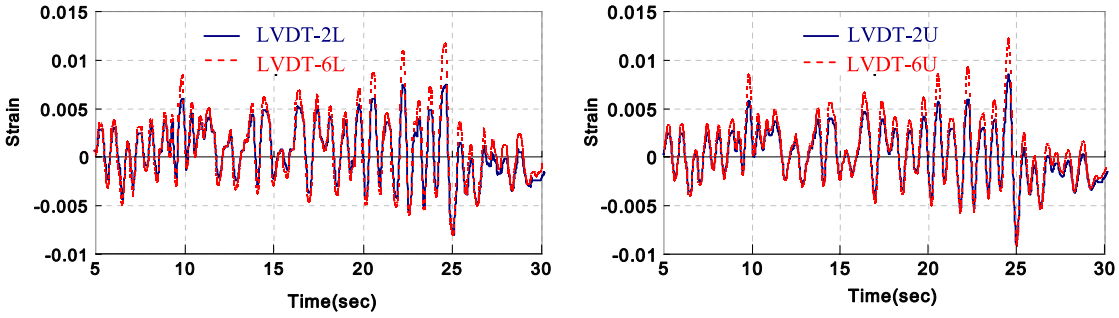

Fig. 32. Measured LVDT responses under the 2/50 event.

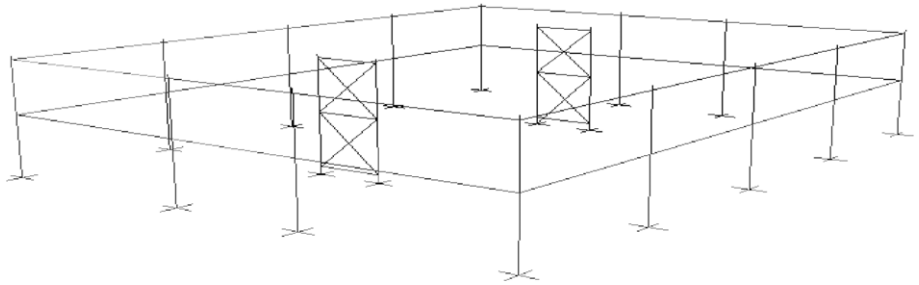

Fig. 33. PISA3D analytical model (equivalent brace model).

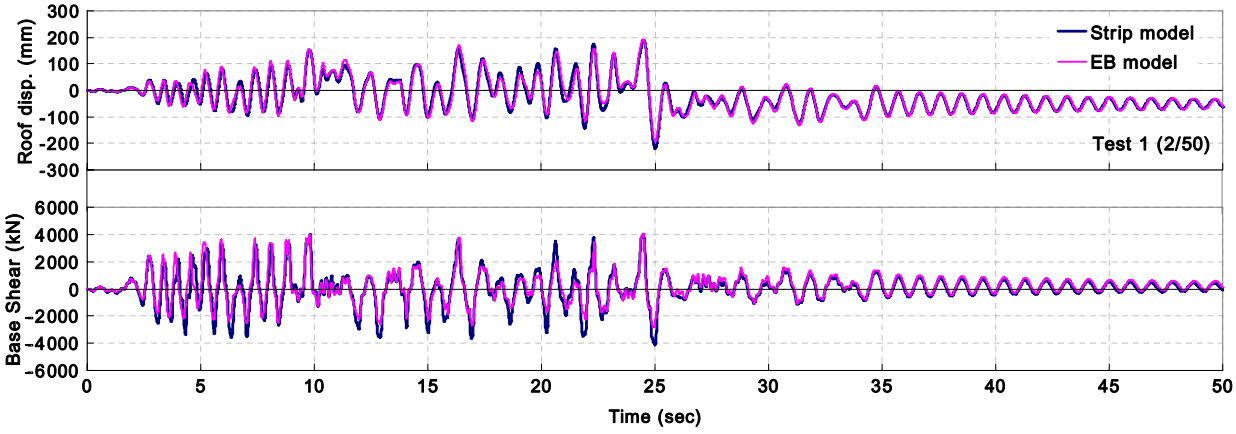

Fig. 34. Roof displacement and base shear time history responses computed from the strip model and the EB model under the 2/50 event.

- The two-story SPSW specimen sustained four earthquake ground motions without failure of the boundary elements. It appears that the proposed simplified capacity design method provides a conservative approach to proportioning the size of boundary elements.
- Tension field action of the infill steel could be developed during a strong earthquake after the steel panel buckled. This would require the SPSW to displace further to stretch the buckled steel panel before the tension field action can be regained. This suggests that, after a strong initial earthquake, the SPSW would have to drift further to resist a second earthquake.
- The strip model can be effectively applied to study the deformation demands imposed on the various parts of the steel infill. The analytical results show that the tension field action is substantially more pronounced in the center of an SPSW than in the corner.
- The yield stress for the equivalent braces can be conveniently computed from the yield stress of the steel panel, the incline angle of the tension strips and the aspect ratio of the steel panel.
- If the boundary elements are properly proportioned following the proposed simplified capacity design principle, the EB model can be used effectively for response analysis of SPSW buildings subjected to strong ground motions.

Acknowledgements

The authors would like to express their appreciation to the laboratory support provided by the technicians at the NCREE. Mr. Kung-Juin Wang was in charge of software development for the networked hybrid test. Dr. Yuan-Tao Weng and Mr. Ying-Cheng Lin assisted in the preparation and execution of the tests. Graduate students Wang-Da Hsieh, Chou-hsieng Li, Ching-Chieh Lin, Te-Hong Lin and Gia-Yuang Liu assisted in the preparation of the tests. Their assistance was essential to the success of the tests. The financial support provided by the Taiwan National Science Council is very much appreciated.

References

[1] Vian D, Bruneau M. Steel plate shear walls for seismic design and retrofit of building structures. Technical report MCEER-05-0010. Buffalo (NY): Multidisciplinary Center for Earthquake Engineering Research; 2005.
[2] Driver RG, Kulak GL, Kennedy DJL, Elwi AE. Cyclic test of four-story steel plate shear wall. Journal of Structural Engineering, ASCE 1998;124(2):112–20.

[3] Timler P, Ventura CE, Prion H, Anjam R. Experimental and analytical studies of steel plate shear walls as applied to the design of tall buildings. The Structural Design of Tall Buildings 1998;7:233–49.
[4] Lubell AS, Prion H, Ventura CE, Rezai M. Unstiffened steel plate shear wall performance under cyclic loading. Journal of Structural Engineering, ASCE 2000;126(4):453–60.
[5] Berman J. Experimental investigation of lightgauge steel plate shear walls for the seismic retrofit of buildings. M.A.Sc. thesis. Department of Civil, Structural, and Environmental Engineering. State University of New York at Buffalo; December 2002.
[6] Berman J, Bruneau M. Plastic analysis and design of steel plate shear walls. Journal of Structural Engineering, ASCE 2003;129(11):1448–56.
[7] Vian D, Lin YC, Bruneau M, Tsai KC. Cyclic performance of low yield strength steel panel shear walls. In: Proceedings of the sixteenth KKCNN symposium on civil engineering. 2003. p. 379–84.
[8] Vian D, Bruneau M, Tsai KC, Lin YC. Special perforated steel plate shear walls with reduced beam section anchor beams I: experimental investigation. ASCE Journal of Structural Engineering 2009;135(3):211–20.
[9] Vian D, Bruneau M, Purba R. Special perforated steel plate shear walls with reduced beam section anchor beams II: analysis and design recommendations. ASCE Journal of Structural Engineering 2009;135(3):221–8.
[10] Tsai KC, Lin CH, Lin YC, Hsieh WD, Qu B. Substructural hybrid tests of a full scale 2-story steel plate shear wall. Technical report NCREE-06-017. National Center for Research on Earthquake Engineering; 2006 [in Chinese].
[11] Thorburn LJ, Kulak GL, Montgomery CJ. Analysis of steel plate shear walls. Structural engineering report no. 107. Edmonton (Alberta, Canada): Department of Civil Engineering. University of Alberta; 1983.
[12] Qu B, Bruneau M, Lin CH, Tsai KC. Testing of full scale two-story steel plate shear wall with reduced beam sections connections and composite floors. Journal of Structural Engineering, ASCE 2008;134(3):364–73.
[13] Shishkin JJ, Driver RG, Grondin GY. Analysis of steel plate shear walls using the modified strip model. Journal of Structural Engineering, ASCE 2009;135(11):1357–66.
[14] Lin YC, Tsai KC. Seismic responses of steel shear wall constructed with restrainers. Technical report NCREE-04-015. Taipei (Taiwan): National Center for Research on Earthquake Engineering; 2004 [in Chinese].
[15] Tsai KC, Lin BZ. User manual for the platform of inelastic structural analysis for 3D systems. PISA3D. Report no. CEER/R92-04. Center for Earthquake Engineering Research. National Taiwan University; 2003.
[16] Li CH, Tsai KC, Lin CH, Chen PC. Cyclic tests of four two-story narrow steel plate shear walls. Part 2: experimental results and design implications. Journal of Earthquake Engineering and Structural Dynamics 2009;39(7):801–26.
[17] Wang KJ, Tsai KC, Wang SJ, Cheng WC, Yang YS. ISEE: Internet-based simulation for earthquake engineering—part II: the application protocol approach. Journal of Earthquake Engineering and Structural Dynamics 2007;36:2307–23.
[18] Manjoine MJ. Influence of rate of strain and temperature on yield stress of mild steel. Journal of Applied Mechanics 1944;11:211–8.